AD-A113 906 ARMY MATERIALS AND MECHANICS RESEARCH CENTER WATERTOWN MA F/G 11/6
ANISOTROPIC EMBRITTLEMENT IN HIGH-HARDNESS ESR 4340 STEEL FORGI--ETC(U)
JAN 82 G B OLSON, A A ANCTIL, T S DESISTO

UNCLASSIFIED AMMRC-TR-82-1 NL

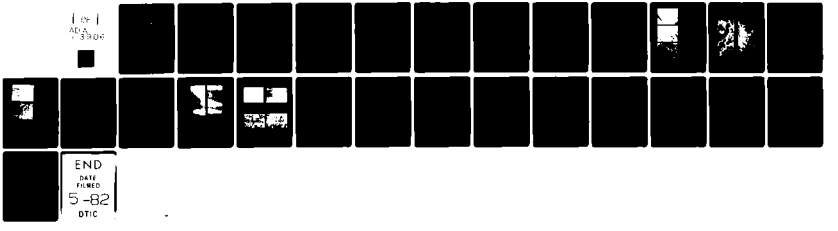

END
DATE FILMED
5-82
DTIC

(12)

AMMRC TR 82-1

AD

ANISOTROPIC EMBRITTLEMENT IN HIGH-HARDNESS ESR 4340 STEEL FORGINGS

GREGORY B. OLSON, ALBERT A. ANCTIL,
THOMAS S. DeSISTO, and ERIC B. KULA
METALS RESEARCH DIVISION

January 1982

ARMY MATERIALS AND MECHANICS RESEARCH CENTER
Watertown, Massachusetts 02172

The findings in this report are not to be construed as an official Department of the Army position, unless so designated by other authorized documents.

Mention of any trade names or manufacturers in this report shall not be construed as advertising nor as an official indorsement or approval of such products or companies by the United States Government.

DISPOSITION INSTRUCTIONS

Destroy this report when it is no longer needed.
Do not return it to the originator.

UNCLASSIFIED

SECURITY CLASSIFICATION OF THIS PAGE (When Data Entered)

REPORT DOCUMENTATION PAGE		READ INSTRUCTIONS BEFORE COMPLETING FORM
1. REPORT NUMBER AMMRC TR 82-1	2. GOVT ACCESSION NO. AD-A113 906	3. RECIPIENT'S CATALOG NUMBER
4. TITLE (and Subtitle) ANISOTROPIC EMBRITTLEMENT IN HIGH-HARDNESS ESR 4340 STEEL FORGINGS		5. TYPE OF REPORT & PERIOD COVERED Final Report 6. PERFORMING ORG. REPORT NUMBER
7. AUTHOR(s) Gregory B. Olson, Albert A. Anctil, Thomas S. DeSisto, and Eric B. Kula		8. CONTRACT OR GRANT NUMBER(s)
9. PERFORMING ORGANIZATION NAME AND ADDRESS Army Materials and Mechanics Research Center Watertown, Massachusetts 02172 DRXMR-MM		10. PROGRAM ELEMENT, PROJECT, TASK AREA & WORK UNIT NUMBERS D/A Project: 1L162105AH84 AMCMS Code: 612105.H840011 Agency Accession:
11. CONTROLLING OFFICE NAME AND ADDRESS U. S. Army Materiel Development and Readiness Command, Alexandria, Virginia 22333		12. REPORT DATE January 1982 13. NUMBER OF PAGES 19
14. MONITORING AGENCY NAME & ADDRESS(if different from Controlling Office)		15. SECURITY CLASS. (of this report) Unclassified 15a. DECLASSIFICATION/DOWNGRADING SCHEDULE

16. DISTRIBUTION STATEMENT (of this Report)

Approved for public release; distribution unlimited.

17. DISTRIBUTION STATEMENT (of the abstract entered in Block 20, if different from Report)

18. SUPPLEMENTARY NOTES

19. KEY WORDS (Continue on reverse side if necessary and identify by block number)

Low alloy steels (4340)	Anisotropy
Electroslag remelting (ESR)	Embrittlement
Mechanical properties	Homogenization

20. ABSTRACT (Continue on reverse side if necessary and identify by block number)

(SEE REVERSE SIDE)

DD FORM 1 JAN 73 1473 EDITION OF 1 NOV 65 IS OBSOLETE

UNCLASSIFIED

SECURITY CLASSIFICATION OF THIS PAGE (When Data Entered)

Block No. 20

ABSTRACT

ESR 4340 steel forgings tempered to a hardness of HRC 55 exhibit a severe loss of tensile ductility in the short transverse direction which is strain-rate and humidity dependent. The anisotropy is also reflected in blunt-notch Charpy impact energy, but is absent in the sharp-crack fracture toughness. Brittle behavior is associated with regions of smooth intergranular fracture which are aligned with microstructural banding. Scanning Auger microprobe analysis indicates some intergranular segregation of phosphorus and sulfur in these regions. The anisotropic embrittlement is attributed to an interaction of nonequilibrium segregation on solidification with local equilibrium segregation at grain boundaries during austenitizing. This produces defective regions of enhanced intergranular impurity segregation which are oriented during forging. The regions are prone to brittle fracture under impact conditions and abnormal sensitivity to environmental attack during low strain-rate deformation. A relatively sparse distribution of these defects (10^2 in.$^{-3}$) accounts for the discrepancy between smooth bar and blunt-notch tests versus sharp-crack tests. Isotropic properties are restored by homogenization treatment. For application of these steels at extreme hardness levels, homogenization treatment is essential.

CONTENTS

INTRODUCTION

Electroslag remelt (ESR) processed 4340 steel tempered to high hardness levels exhibits superior ballistic properties,[1,2] attributed primarily to the improved shatter resistance accompanying a low sulfide inclusion content. This improved ballistic performance led to the selection of ESR 4340 steel tempered to HRC 55 hardness for ballistically-tolerant critical helicopter components. Preliminary mechanical property evaluation at AMMRC of commercial ESR 4340 steel forgings revealed a severe loss of ductility in the short transverse direction;* this was followed by a number of delayed failures of helicopter components in service. This study was undertaken to determine the nature and mechanism of the severe degradation of short transverse mechanical properties in the high hardness ESR 4340 steel forgings.

MATERIALS AND EXPERIMENTAL PROCEDURES

Material from sixteen ESR 4340 forgings from nine commercial heats produced by three suppliers was evaluated. Also included were an ESR 300M (Si-modified 4340) heat and one VIM 4340 heat for comparison. The forgings are identified in Table 1 and heat analyses are given in Table 2. Original ESR ingots were generally 20 inches in diameter. Particular deviations in heat compositions are noted in Table 1. Unless otherwise indicated, specimens were normalized at 1650°F for 1 hour and air cooled, austenitized at 1550°F for 1 hour and oil quenched, and tempered at 340°F for 1 hour as per helicopter component specifications.

Tension tests were conducted on standard 0.252-in.-diameter specimens with a 1.25-in. reduced section and 1.0-in. gage length at a crosshead speed of 0.05 in./min. Fracture toughness was evaluated both by standard Charpy impact tests and slow-bend tests on precracked Charpy specimens; sharp-crack fracture toughness (K_{IC}) values were estimated from maximum load measurements using a Manlabs, Inc. Physmet Slow-Bend tester.

Table 1. FORGING IDENTIFICATION

Heat No.	Alloy	Producer Heat No.	Forgings	Remarks
A1	ESR 4340	L-R0210	3" plate	0.06 Sn
A2		L-R0310	3" plate	0.06 Sn
A3		L-R0353	3" plate	-
A4		L-1700	2.5" plate	-
B1		C-G712	a. 7"x7", b. 5"x5", c. [illegible]x3"	0.012 P, 0.0075 S
B2		C-G721	a. 5"x7", b. 5"x5", c. [illegible]x5"	30 ppm H
C1		S-BM2	a. 12½" sq, b. 11"x12", c. 5"x12"	-
C2		S-GIT.4	4" plate	0.010 P
C3	↓	S-9060-2	4-3/4" round	7 ppm H
D	ESR 300M	B-RM 355	6"x4"	-
E	VIM 4340	A-A10	6"x4"	-

*ANCTIL, A. A., DeSISTO, T. S., and KULA, E. B. Army Materials and Mechanics Research Center, unpublished research, 1978.

1. HICKEY, C. F., Jr., ANCTIL, A. A., and CHAIT, R. *The Ballistic Performance of High Strength 4340 Steel Processed by Electroslag Remelting* in Fracture Toughness of Wrought and Cast Steels, ed. F. Fortner, ASMI MPC-13, 1980, p. 219-229
2. ROHTERT, R. E. *Ballistic Design Support Tests - A Tool for Helicopter Vulnerability Reduction* 31st Annual National Forum of the American Helicopter Society, preprint 984, Washington, D.C., May 1975

Table 2. CHEMICAL COMPOSITIONS

Heat No.	Weight Percent													ppm	
	C	Mn	Si	Ni	Cr	Mo	P	S	Cu	N	As	Sb	Sn	O	H
A1	0.40	0.79	0.24	1.71	0.69	0.19	0.005	0.002	0.14	0.017	0.006	0.003	0.060	7	0.2
A2	0.38	0.77	0.22	1.68	0.74	0.22	0.007	0.003	*	0.008	0.010	0.005	0.060	15	2.0
A3	0.36	0.74	0.26	1.80	0.77	0.26	0.007	0.001	*	0.011	0.009	0.004	0.005	6	1.4
A4	0.41	0.73	0.32	1.85	0.73	0.23	0.007	0.002	0.20	0.011	0.009	0.004	0.005	14	0.4
B1	0.43	0.72	0.35	1.83	0.90	0.31	0.012	0.007	0.25	0.012	0.010	0.003	0.006	26	0.3
B2	0.42	0.72	0.34	1.88	0.85	0.29	0.009	0.004	*	0.008	0.009	0.003	0.005	30	0.5
C1	0.40	0.77	0.22	1.78	0.80	0.24	0.008	0.003	*	0.010	0.013	0.002	0.014	16	0.6
C2	0.40	0.77	0.20	1.69	0.85	0.24	0.010	0.003	*	0.013	0.006	0.004	0.016	11	0.1
C3	0.43	0.80	0.29	1.77	0.80	0.26	0.005	0.004	0.09	0.010	0.004	0.001	0.003	41	7.0
D	0.40	0.87	1.61	1.83	0.77	0.36	0.008	0.006	0.13	0.009	0.024	*	0.018	*	*
E	0.39	0.96	0.28	2.02	0.80	0.28	0.007	0.002	0.07	0.007	0.008	0.004	0.010	23	0.4

*Was not determined

Fracture surfaces were analyzed on notched specimens fractured in vacuum in a PHI Electronics Scanning Auger Electron Microprobe operated at 3 kV. Some controlled humidity smooth bar tension tests were run on standard 0.160-in.-dia. specimens in a specially designed environmental chamber. Short transverse K_{ISCC} tests were conducted in 3-1/2% NaCl solution using constant load SEN precracked specimens with electron-beam welded grip ends.

MECHANICAL PROPERTIES

Table 3 summarizes the results of extensive mechanical testing. Properties were measured in the longitudinal (L), long transverse (LT), and short transverse (ST) directions of the forgings.* Tensile properties represent average values over the number of tension tests indicated; numbers of toughness tests are indicated in parentheses. Longitudinal properties are typical of 4340 steel of this hardness level, but transverse properties reveal substantial anisotropy. While some anisotropy is evident in the tensile strength and total elongation (in 1.0 in.), the most dramatic effect is found in the tensile reduction of area, where zero values often associated with brittle fracture outside the gage section are frequently observed in the short transverse direction. The anisotropy is generally more pronounced as the degree of forging reduction is increased. Significant anisotropy is also evident in the blunt-notch impact toughness as measured by the Charpy (C_V) energy, while the sharp-crack toughness measured by K_{IC} shows little sensitivity to the test direction. Results for the ESR 300M and VIM 4340 are consistent with the same trends.

The influence of tempering temperature on the short transverse tensile properties was investigated in heats A1, A2, and A3; the results are presented in Table 4 and plotted in Figure 1. Tempering to a lower strength level is found to quickly restore ductility in heat A3. The effect is more gradual in heats A1 and A2 which have an abnormal Sn content. While such abnormal impurity contents appear to aggravate the problem, substantial anisotropy is present after the 340°F temper in heats which show no such composition abnormalities.

*The transverse direction is identified as T in symmetric forgings.

Table 3. MECHANICAL PROPERTIES OF ESR 4340 STEEL TEMPERED AT 340 F FOR 1 HOUR

Heat No.	Forging	Direction	N	0.2% YS, ksi	UTS, ksi	Elon., %	RA, %	CV (N), ft-lb	K_{IC} (N) ksi$\sqrt{in.}$	HRC
A1	3" plate	L	2	209	308	11.3	33.4	17.8 (1)	36.9 (7)	56
		LT	4	210	239	5.9	7.6	-	-	-
		ST	2	206	186	1.5	0	5.0 (1)	38.0 (4)	56
A2	3" plate	ST	2	-	188	0	0	-	-	-
A3	3" plate	ST	2	214	281	0	0	-	-	-
A4[a]	2.5" plate	L	2	229	288	13	43.2	17.5 (2)	-	53
		LT	2	229	288	11	33.7	12.9 (2)	-	53
		ST	4	227	287	5.5	12.3	6.6[b](4)	-	53
B1	a. 7"x7"	L	4	218	305	6.3	15.5	12.5 (2)	42.9 (2)	56
		T	10	215	219	0.4	0.6	10.9 (5)	40.2 (5)	56
	b. 5"x5"	L	4	212	317	9.6	37.1	12.4 (2)	40.3 (2)	56
		T	10	217	244	2.9	4.8	8.8 (5)	39.8 (5)	56
	c. 3"x3"	L	4	210	329	12.1	37.6	12.3 (2)	37.0 (2)	57
		T	10	-	252	3.3	5.9	9.2 (5)	33.8 (5)	57
B2	a. 5"x7"	L	2	210	317	8.0	21.1	17.5 (1)	54.3 (1)	57
		ST	5	220	297	5.0	14.9	8.8 (3)	45.6 (2)	57
	b. 5"x5"	L	2	211	320	12.5	38.9	10.9 (1)	55.1 (1)	57
		ST	4	222	319	9.3	22.6	12.1 (2)	50.9 (2)	57
	c. 3"x5"	L	2	213	320	12.0	38.6	15.5 (1)	50.1 (1)	57
		ST	4	220	322	7.5	19.5	11.4 (2)	54.5 (2)	57
C1	a. 12½"x12½"	L	4	-	301	13.0	43.3	14.6 (4)	-	54
		T	8	213	297	13.5	42.9	15.2 (8)	-	54
	b. 11"x12"	L	2	217	300	13.0	44.6	14.1 (2)	-	55
		T	4	214	297	12.4	37.9	13.8 (4)	-	55
	c. 5"x12"	LT	8	213	302	13.4	41.9	14.0 (4)	-	55
		ST	15	210	274	6.0	14.5	10.1 (4)	45.8 (4)	55
	d. 3¼"x3¼" 2300°F[c] (from 5"x6" of C1-a)	T	4	211	304	14.4	47.6	17.1 (2)	56.4 (2)	55
		ST	10	210	304	12.3	39.2	14.8 (5)	53.1 (5)	55
C2	0.4" plate	L	8	214	304	12.0	49.1	18.7 (4)	51.4 (4)	55
		LT	8	212	305	10.6	43.4	19.2 (4)	52.7 (4)	55
C3[d]	4-3/4" round	L	3	198	315	11.0	35.5	12.1 (4)	-	55
		T	6	201	316	9.0	25.7	8.8 (6)	-	55
D[e]	300M 4"x6"	L	8	245	291	10.6	44.2	19.7 (4)	-	55
		LT	8	252	295	7.8	30.2	14.7 (4)	-	55
		ST	8	246	293	5.9	19.9	11.2 (4)	-	55
E	VIM 4340 4"x6"	L	8	217	308	12.0	46.2	20.0 (4)	-	55
		LT	8	205	309	9.3	29.6	14.0 (4)	-	55
		ST	8	212	307	7.9	23.3	13.8 (4)	-	54

a - 400°F temper
b - Intergranular fracture
c - AMMRC forged
d - Tempered 4 hours
e - 570°F temper

Considerable scatter is found to accompany the low short transverse ductility after 340°F tempering with some indication of a specimen size dependence. Of the fifteen ST tension specimens of forging c (5"x12") of heat C1 cited in Table 3, seven specimens were of 0.160-in. dia. with a 1.0-in. reduced section. The eight standard 0.252-in.-dia. specimens showed an average RA of 1.5%, with five specimens giving 0 values, and one showing a "normal" value of 41. The smaller 0.160-in.-dia. specimens gave a higher average RA of 22.4% with a range of 5.5% to 43.1%. The standard deviation was 14 for both specimen sizes. As the two sizes were tested at different times, uncontrolled variables such as humidity might contribute to these differences, as will be discussed later.

Table 4. INFLUENCE OF TEMPERING TEMPERATURE ON SHORT-TRANSVERSE TENSILE PROPERTIES $\dot{\varepsilon} = 0.05\ min^{-1}$

Heat No.	Temper, °F	0.2% YS, ksi	UTS, ksi	% Elon.	% RA
A1	340	206*	186±24	1.5±1.5	0
	400	234*	219±15	0.5	0.8
	500	234*	249±16	3.5±1.5	7.8±6.8
	600	228	252	4.0±1.0	6.8±0.4
	800	207	218	8.2±0.2	23.3±3.5
	1000	172	180	10.5±0.5	30.5±1.7
	1200	126	139	18.5±1.5	48.0
A2	340	-	188±18	0	0
	500	222	265±4	0	1.8
	600	226	256	7.5±1.0	18.4±2.8
	800	208	218	7.0	17.7
	1000	180±2	186	11.2±0.2	32.1±1.3
	1200	134	146	16.0±0.5	44.3±0.9
A3	340	214±2	267	0	1.3±1.3
	500	222±2	270	9.5±0.5	30.8±0.6
	600	228±4	253±2	10.0	33.4±0.6
	800	209±1	219±1	11.5±0.5	36.3±0.9
	1000	182	189	13.5	45.7±0.5
	1200	150	157	19.0	50.6±0.2

Note: One hour temper
Two specimens tested for each condition

*One specimen failed before 0.2% yield

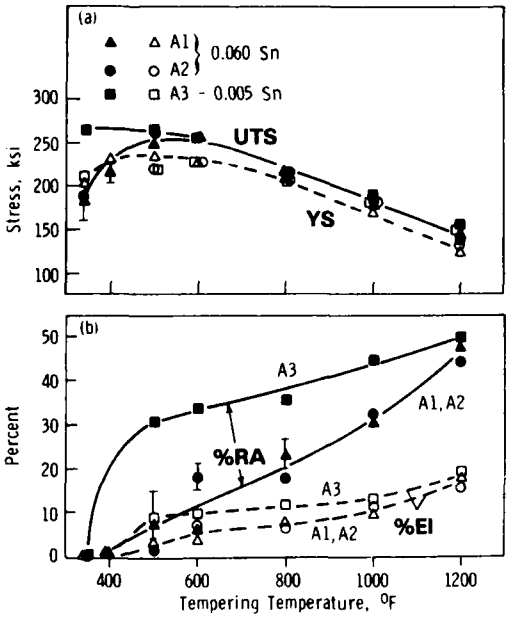

Figure 1. Influence of tempering temperature on short-transverse tensile properties of heats A1, A2, and A3.

Fractography revealed that very low short transverse ductility was generally related to intergranular crack initiation at the specimen surface. Typical scanning electron micrographs are shown in Figure 2.* A region of smooth intergranular fracture, generally 0.01 in. in extent, was always found adjacent to a free surface, while the remainder of the fracture surface showed a ductile mode of fracture by void coalescence. Evidence for intergranular fracture was also commonly observed in the plastic zone of the Charpy bars, with secondary intergranular cracks tending to follow the

*Fractures occasionally initiated at MnS stringers located near the specimen surface without significant intergranular fracture; specimens exhibiting the lowest ductilities, however, invariably showed intergranular initiation.

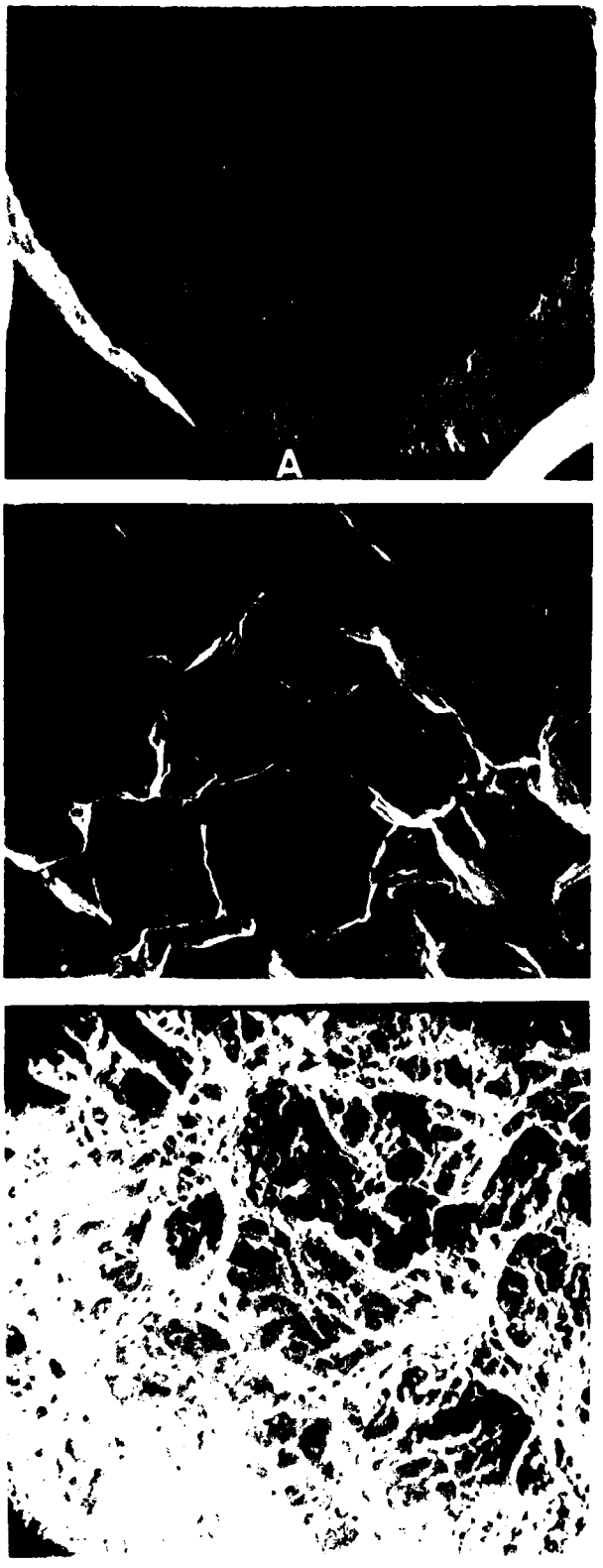

Figure 2. Scanning electron micrographs of fracture surface of short-transverse tension specimen of C1-c material. (a) Overall view showing flat fracture mode at failure origin "A," (b) smooth intergranular fracture at failure origin, and (c) ductile fracture mode at specimen center.

rolling plane. Figure 3 shows optical micrographs of such secondary cracking in the a and b forgings of heat C1. The plane of polish is 0.02 in. below the primary fracture surface of long transverse impact specimens. To assess the possibility that embrittlement might be related to "overheating" during forging,[3] a 5"x6" section of the C1-a material was forged to 3-1/4-in. square at 2300°F. After the standard heat treatment, this high temperature forging, C1-d, was found to show improved mechanical properties (Table 3) rather than further embrittlement. As the smooth intergranular fracture initiation at tension specimen surfaces is suggestive of environmentally induced fracture, the influence of strain rate on the short transverse ductility was investigated

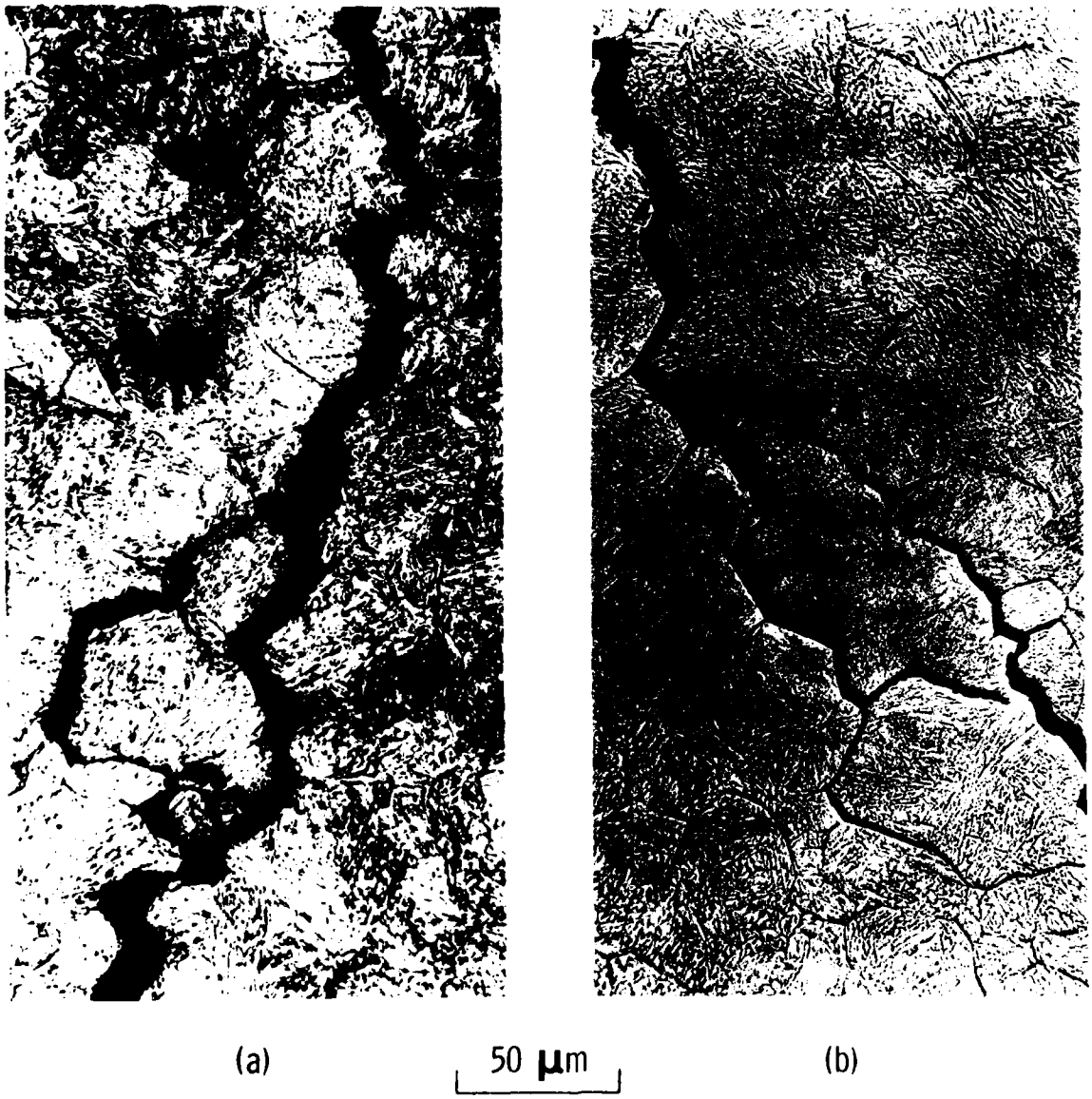

Figure 3. Secondary intergranular cracking in long-transverse Charpy specimens from heat C1, forgings a and b.

3. ANDREW, R. C., WESTON, G. M., and SOUTHIN, R. T. *Overheating in Low Sulfur Steels.* J. Australasian Inst. Metals, v. 21, 1976, p. 126-131.

in 0.160-in.-dia. specimens of the C1-c forging, giving the results shown in Figure 4. Lower strain rate clearly reduces the ductility. Also included in Figure 4 are the results of low strain-rate tests run in vacuum after thoroughly washing the specimens in alcohol. A normal level of ductility is restored under these conditions, clearly demonstrating that the abnormal short transverse ductility is associated with an environmental interaction or "stress-corrosion" phenomenon.

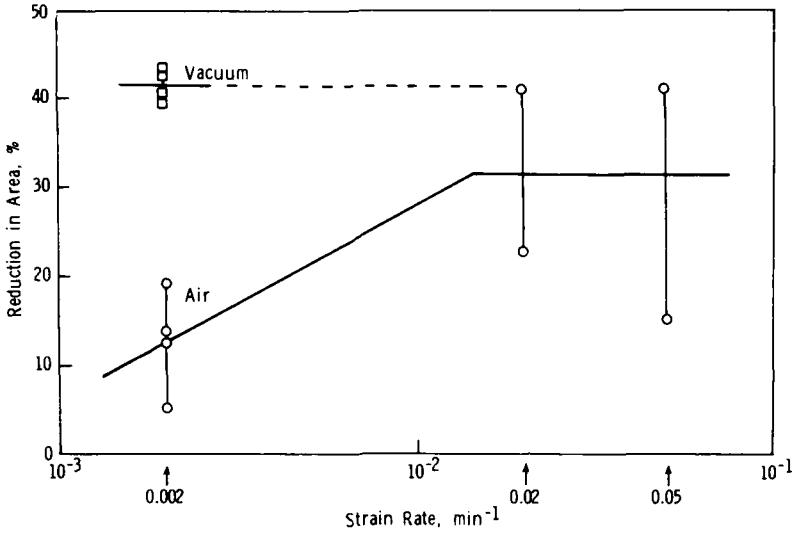

Figure 4. Strain-rate dependence of short-transverse tensile ductility of C1-c forging tested in laboratory air. Ductility in vacuum at lowest rate is also shown.

SEGREGATION BEHAVIOR

In accordance with commercial practice, none of the ingots or forgings was given a high temperature homogenization treatment at any stage of processing. Macroetched specimens showed a typical "banded" structure as illustrated by the Al 3-in. plate shown in Figure 5; a higher magnification micrograph is shown in Figure 6.

To assess the possible relation between banding and crack initiation, prepolished and etched bend specimens of the C1-c material were stressed in the short transverse direction. Small cracks generally followed dark bands when observed under oblique illumination as shown in Figure 7. Comparison with the appearance of identically etched and illuminated as-cast 4340 steel indicated that the dark areas correspond to the interdendritic regions of the original ingot structure. A study of banding in 4340 steel by Rao[4] has demonstrated that these regions are enriched in alloy elements (Mn, Cr, Ni, and Mo) as well as impurities, notably phosphorus and sulfur.

In order to evaluate segregation at grain boundaries, short transverse notched 3-mm-dia. bars of the C1-c material were fractured in the vacuum system of a Scanning Auger Electron Microprobe (SAM). Despite the frequent observation of intergranular fracture in Charpy impact specimens (as in Figure 3), no clear examples of intergranular

4. RAO, A. V. *Banding and Its Influence on the Impact and Fatigue Properties of High Strength SAE 4340 Steel.* PhD Thesis, Dept. of Metallurgy, Mechanics and Mat. Sci., Michigan State University, 1973.

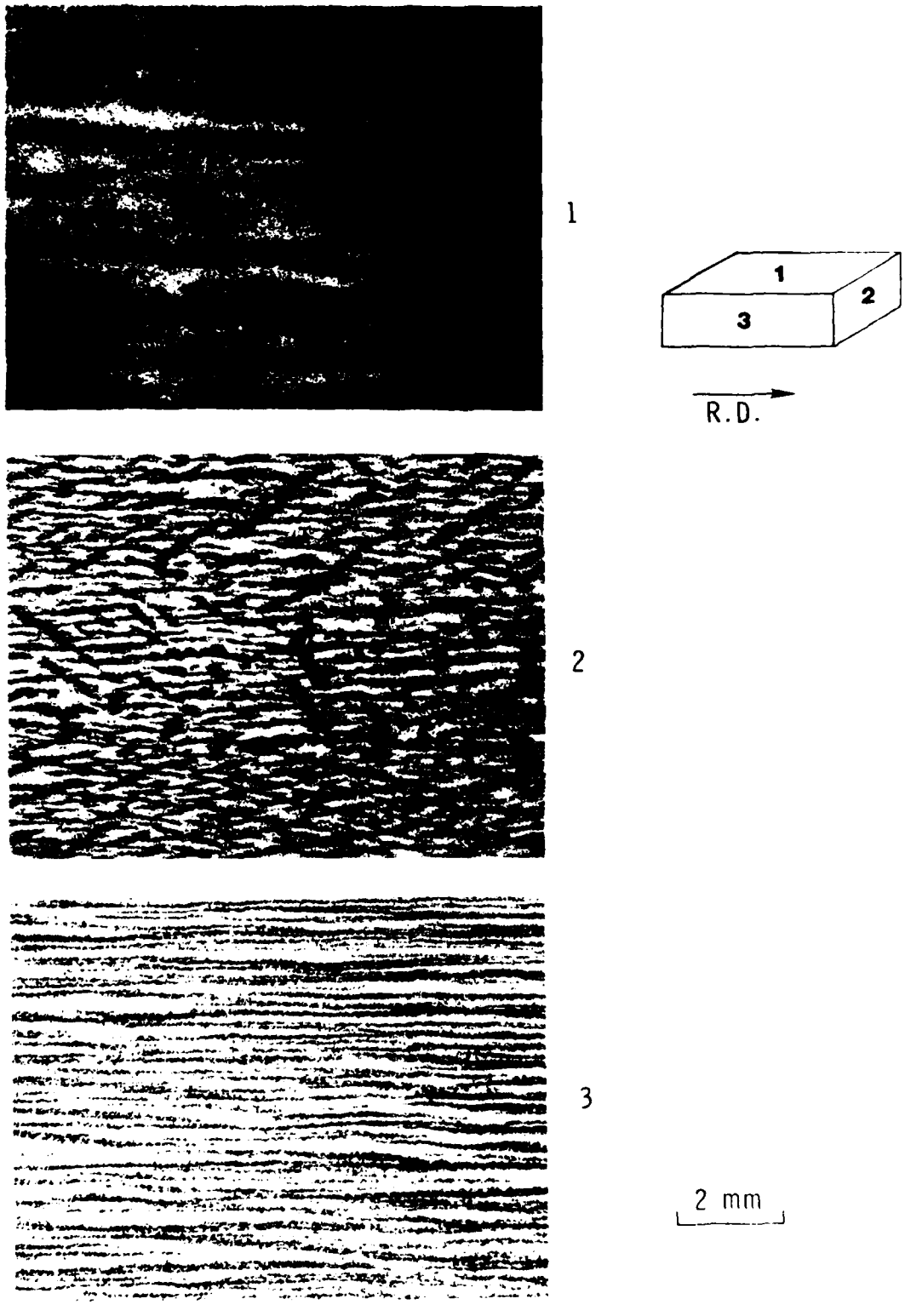

Figure 5. Banded structure of A1 material revealed by macro-etching with Oberhoffer's reagent.

Army Materials and Mechanics Research Center,
Watertown, Massachusetts 02172
ANISOTROPIC EMBRITTLEMENT IN HIGH-HARDNESS ESR 4340 STEEL FORGINGS -
Gregory B. Olson, Albert A. Anctil, Thomas DeSisto, and Eric B. Kula

Technical Report AMMRC TR 82-1, January 1982, 19 pp - illus-tables, D/A Project 1L162105AH84, AMCMS Code 612105.H840011

AD ______________

UNCLASSIFIED
UNLIMITED DISTRIBUTION

Key Words

Low alloy steels (4340)
Electroslag remelting (ESR)
Mechanical properties

ESR 4340 steel forgings tempered to a hardness of HRC 55 exhibit a severe loss of tensile ductility in the short transverse direction which is strain-rate and humidity dependent. The anisotropy is also reflected in blunt-notch Charpy impact energy, but is absent in the sharp-crack fracture toughness. Brittle behavior is associated with regions of smooth intergranular fracture which are aligned with microstructural banding. Scanning Auger microprobe analysis indicates some intergranular segregation of phosphorus and sulfur in these regions. The anisotropic embrittlement is attributed to an interaction of nonequilibrium segregation on solidification with local equilibrium segregation at grain boundaries during austenitizing. This produces defective regions of enhanced intergranular impurity segregation which are oriented during forging. The regions are prone to brittle fracture under impact conditions and abnormal sensitivity to environmental attack during low strain-rate deformation. A relatively sparse distribution of these defects (10^2 in.$^{-3}$) accounts for the discrepancy between smooth bar and blunt-notch tests versus sharp-crack tests. Isotropic properties are restored by homogenization treatment. For application of these steels at extreme hardness levels, homogenization treatment is essential.

Army Materials and Mechanics Research Center,
Watertown, Massachusetts 02172
ANISOTROPIC EMBRITTLEMENT IN HIGH-HARDNESS ESR 4340 STEEL FORGINGS -
Gregory B. Olson, Albert A. Anctil, Thomas DeSisto, and Eric B. Kula

Technical Report AMMRC TR 82-1, January 1982, 19 pp - illus-tables, D/A Project 1L162105AH84, AMCMS Code 612105.H840011

AD ______________

UNCLASSIFIED
UNLIMITED DISTRIBUTION

Key Words

Low alloy steels (4340)
Electroslag remelting (ESR)
Mechanical properties

ESR 4340 steel forgings tempered to a hardness of HRC 55 exhibit a severe loss of tensile ductility in the short transverse direction which is strain-rate and humidity dependent. The anisotropy is also reflected in blunt-notch Charpy impact energy, but is absent in the sharp-crack fracture toughness. Brittle behavior is associated with regions of smooth intergranular fracture which are aligned with microstructural banding. Scanning Auger microprobe analysis indicates some intergranular segregation of phosphorus and sulfur in these regions. The anisotropic embrittlement is attributed to an interaction of nonequilibrium segregation on solidification with local equilibrium segregation at grain boundaries during austenitizing. This produces defective regions of enhanced intergranular impurity segregation which are oriented during forging. The regions are prone to brittle fracture under impact conditions and abnormal sensitivity to environmental attack during low strain-rate deformation. A relatively sparse distribution of these defects (10^2 in.$^{-3}$) accounts for the discrepancy between smooth bar and blunt-notch tests versus sharp-crack tests. Isotropic properties are restored by homogenization treatment. For application of these steels at extreme hardness levels, homogenization treatment is essential.

Army Materials and Mechanics Research Center,
Watertown, Massachusetts 02172
ANISOTROPIC EMBRITTLEMENT IN HIGH-HARDNESS ESR 4340 STEEL FORGINGS -
Gregory B. Olson, Albert A. Anctil, Thomas DeSisto, and Eric B. Kula

Technical Report AMMRC TR 82-1, January 1982, 19 pp - illus-tables, D/A Project 1L162105AH84, AMCMS Code 612105.H840011

AD ______________

UNCLASSIFIED
UNLIMITED DISTRIBUTION

Key Words

Low alloy steels (4340)
Electroslag remelting (ESR)
Mechanical properties

ESR 4340 steel forgings tempered to a hardness of HRC 55 exhibit a severe loss of tensile ductility in the short transverse direction which is strain-rate and humidity dependent. The anisotropy is also reflected in blunt-notch Charpy impact energy, but is absent in the sharp-crack fracture toughness. Brittle behavior is associated with regions of smooth intergranular fracture which are aligned with microstructural banding. Scanning Auger microprobe analysis indicates some intergranular segregation of phosphorus and sulfur in these regions. The anisotropic embrittlement is attributed to an interaction of nonequilibrium segregation on solidification with local equilibrium segregation at grain boundaries during austenitizing. This produces defective regions of enhanced intergranular impurity segregation which are oriented during forging. The regions are prone to brittle fracture under impact conditions and abnormal sensitivity to environmental attack during low strain-rate deformation. A relatively sparse distribution of these defects (10^2 in.$^{-3}$) accounts for the discrepancy between smooth bar and blunt-notch tests versus sharp-crack tests. Isotropic properties are restored by homogenization treatment. For application of these steels at extreme hardness levels, homogenization treatment is essential.

Army Materials and Mechanics Research Center,
Watertown, Massachusetts 02172
ANISOTROPIC EMBRITTLEMENT IN HIGH-HARDNESS ESR 4340 STEEL FORGINGS -
Gregory B. Olson, Albert A. Anctil, Thomas DeSisto, and Eric B. Kula

Technical Report AMMRC TR 82-1, January 1982, 19 pp - illus-tables, D/A Project 1L162105AH84, AMCMS Code 612105.H840011

AD ______________

UNCLASSIFIED
UNLIMITED DISTRIBUTION

Key Words

Low alloy steels (4340)
Electroslag remelting (ESR)
Mechanical properties

ESR 4340 steel forgings tempered to a hardness of HRC 55 exhibit a severe loss of tensile ductility in the short transverse direction which is strain-rate and humidity dependent. The anisotropy is also reflected in blunt-notch Charpy impact energy, but is absent in the sharp-crack fracture toughness. Brittle behavior is associated with regions of smooth intergranular fracture which are aligned with microstructural banding. Scanning Auger microprobe analysis indicates some intergranular segregation of phosphorus and sulfur in these regions. The anisotropic embrittlement is attributed to an interaction of nonequilibrium segregation on solidification with local equilibrium segregation at grain boundaries during austenitizing. This produces defective regions of enhanced intergranular impurity segregation which are oriented during forging. The regions are prone to brittle fracture under impact conditions and abnormal sensitivity to environmental attack during low strain-rate deformation. A relatively sparse distribution of these defects (10^2 in.$^{-3}$) accounts for the discrepancy between smooth bar and blunt-notch tests versus sharp-crack tests. Isotropic properties are restored by homogenization treatment. For application of these steels at extreme hardness levels, homogenization treatment is essential.

Army Materials and Mechanics Research Center,
Watertown, Massachusetts 02172
ANISOTROPIC EMBRITTLEMENT IN HIGH-HARDNESS ESR 4340 STEEL FORGINGS -
Gregory B. Olson, Albert A. Anctil, Thomas DeSisto, and Eric B. Kula

Technical Report AMMRC TR 82-1, January 1982, 19 pp - illus-tables, D/A Project 1L162105AH84, AMCMS Code 612105.H840011

AD ____________

UNCLASSIFIED
UNLIMITED DISTRIBUTION

Key Words

Low alloy steels (4340)
Electroslag remelting (ESR)
Mechanical properties

ESR 4340 steel forgings tempered to a hardness of HRC 55 exhibit a severe loss of tensile ductility in the short transverse direction which is strain-rate and humidity dependent. The anisotropy is also reflected in blunt-notch Charpy impact energy, but is absent in the sharp-crack fracture toughness. Brittle behavior is associated with regions of smooth intergranular fracture which are aligned with microstructural banding. Scanning Auger microprobe analysis indicates some intergranular segregation of phosphorus and sulfur in these regions. The anisotropic embrittlement is attributed to an interaction of nonequilibrium segregation on solidification with local equilibrium segregation at grain boundaries during austenitizing. This produces defective regions of enhanced intergranular impurity segregation which are oriented during forging. The regions are prone to brittle fracture under impact conditions and abnormal sensitivity to environmental attack during low strain-rate deformation. A relatively sparse distribution of these defects (10^2 in.$^{-3}$) accounts for the discrepancy between smooth bar and blunt-notch tests versus sharp-crack tests. Isotropic properties are restored by homogenization treatment. For application of these steels at extreme hardness levels, homogenization treatment is essential.

Army Materials and Mechanics Research Center,
Watertown, Massachusetts 02172
ANISOTROPIC EMBRITTLEMENT IN HIGH-HARDNESS ESR 4340 STEEL FORGINGS -
Gregory B. Olson, Albert A. Anctil, Thomas DeSisto, and Eric B. Kula

Technical Report AMMRC TR 82-1, January 1982, 19 pp - illus-tables, D/A Project 1L162105AH84, AMCMS Code 612105.H840011

AD ____________

UNCLASSIFIED
UNLIMITED DISTRIBUTION

Key Words

Low alloy steels (4340)
Electroslag remelting (ESR)
Mechanical properties

ESR 4340 steel forgings tempered to a hardness of HRC 55 exhibit a severe loss of tensile ductility in the short transverse direction which is strain-rate and humidity dependent. The anisotropy is also reflected in blunt-notch Charpy impact energy, but is absent in the sharp-crack fracture toughness. Brittle behavior is associated with regions of smooth intergranular fracture which are aligned with microstructural banding. Scanning Auger microprobe analysis indicates some intergranular segregation of phosphorus and sulfur in these regions. The anisotropic embrittlement is attributed to an interaction of nonequilibrium segregation on solidification with local equilibrium segregation at grain boundaries during austenitizing. This produces defective regions of enhanced intergranular impurity segregation which are oriented during forging. The regions are prone to brittle fracture under impact conditions and abnormal sensitivity to environmental attack during low strain-rate deformation. A relatively sparse distribution of these defects (10^2 in.$^{-3}$) accounts for the discrepancy between smooth bar and blunt-notch tests versus sharp-crack tests. Isotropic properties are restored by homogenization treatment. For application of these steels at extreme hardness levels, homogenization treatment is essential.

Army Materials and Mechanics Research Center,
Watertown, Massachusetts 02172
ANISOTROPIC EMBRITTLEMENT IN HIGH-HARDNESS ESR 4340 STEEL FORGINGS -
Gregory B. Olson, Albert A. Anctil, Thomas DeSisto, and Eric B. Kula

Technical Report AMMRC TR 82-1, January 1982, 19 pp - illus-tables, D/A Project 1L162105AH84, AMCMS Code 612105.H840011

AD ____________

UNCLASSIFIED
UNLIMITED DISTRIBUTION

Key Words

Low alloy steels (4340)
Electroslag remelting (ESR)
Mechanical properties

ESR 4340 steel forgings tempered to a hardness of HRC 55 exhibit a severe loss of tensile ductility in the short transverse direction which is strain-rate and humidity dependent. The anisotropy is also reflected in blunt-notch Charpy impact energy, but is absent in the sharp-crack fracture toughness. Brittle behavior is associated with regions of smooth intergranular fracture which are aligned with microstructural banding. Scanning Auger microprobe analysis indicates some intergranular segregation of phosphorus and sulfur in these regions. The anisotropic embrittlement is attributed to an interaction of nonequilibrium segregation on solidification with local equilibrium segregation at grain boundaries during austenitizing. This produces defective regions of enhanced intergranular impurity segregation which are oriented during forging. The regions are prone to brittle fracture under impact conditions and abnormal sensitivity to environmental attack during low strain-rate deformation. A relatively sparse distribution of these defects (10^2 in.$^{-3}$) accounts for the discrepancy between smooth bar and blunt-notch tests versus sharp-crack tests. Isotropic properties are restored by homogenization treatment. For application of these steels at extreme hardness levels, homogenization treatment is essential.

Army Materials and Mechanics Research Center,
Watertown, Massachusetts 02172
ANISOTROPIC EMBRITTLEMENT IN HIGH-HARDNESS ESR 4340 STEEL FORGINGS -
Gregory B. Olson, Albert A. Anctil, Thomas DeSisto, and Eric B. Kula

Technical Report AMMRC TR 82-1, January 1982, 19 pp - illus-tables, D/A Project 1L162105AH84, AMCMS Code 612105.H840011

AD ____________

UNCLASSIFIED
UNLIMITED DISTRIBUTION

Key Words

Low alloy steels (4340)
Electroslag remelting (ESR)
Mechanical properties

ESR 4340 steel forgings tempered to a hardness of HRC 55 exhibit a severe loss of tensile ductility in the short transverse direction which is strain-rate and humidity dependent. The anisotropy is also reflected in blunt-notch Charpy impact energy, but is absent in the sharp-crack fracture toughness. Brittle behavior is associated with regions of smooth intergranular fracture which are aligned with microstructural banding. Scanning Auger microprobe analysis indicates some intergranular segregation of phosphorus and sulfur in these regions. The anisotropic embrittlement is attributed to an interaction of nonequilibrium segregation on solidification with local equilibrium segregation at grain boundaries during austenitizing. This produces defective regions of enhanced intergranular impurity segregation which are oriented during forging. The regions are prone to brittle fracture under impact conditions and abnormal sensitivity to environmental attack during low strain-rate deformation. A relatively sparse distribution of these defects (10^2 in.$^{-3}$) accounts for the discrepancy between smooth bar and blunt-notch tests versus sharp-crack tests. Isotropic properties are restored by homogenization treatment. For application of these steels at extreme hardness levels, homogenization treatment is essential.

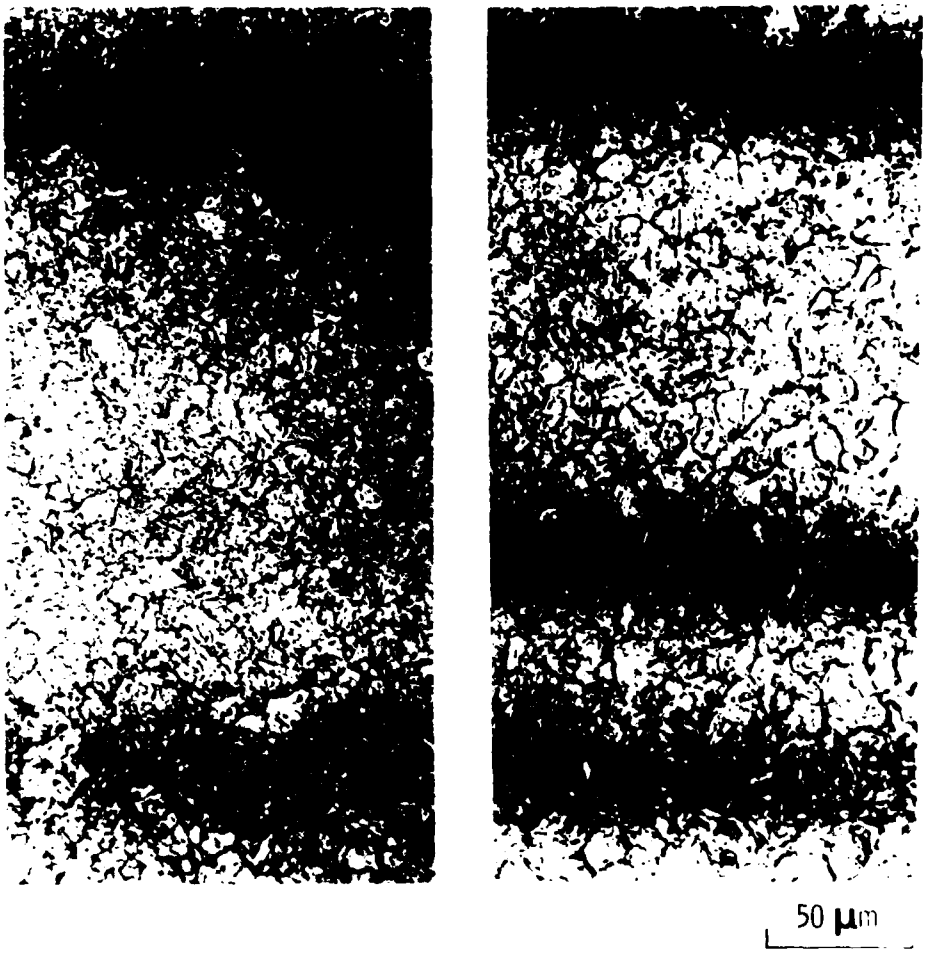

Figure 6. Mid-thickness microstructures of A1 forging. (Etch = 1g sodium tridecylbenzene, 2 drops HCl, 100 cc sat. Picric acid in H_2O).

fracture could be found in the 3-mm specimens, presumably due to a sparse distribution of the defects with which the observed intergranular fracture is associated. Some intergranular fracture could be observed after a grain-coarsening austenitizing treatment at 2200°F. Auger electron analysis of these regions indicated preferential segregation of phosphorus and sulfur, relative to the rest of the fracture surface.

To induce intergranular fracture in the fine-grained conventionally heat-treated material, U-notched specimens were electrolytically hydrogen charged and cadmium plated; the treatment produced internal hydrogen blisters. After fracturing the specimens in the vacuum system, regions of intergranular fracture were found adjacent to the blisters, as shown in Figure 8. Analysis of such regions indicated small amounts of phosphorus and sulfur segregation. The example shown in Figure 9 gives ratios of the P and S peaks to the 704 eV Fe peak of $P_{120}/Fe_{704}=3.1\times10^{-3}$ and $S_{152}/Fe_{704}=1.7\times10^{-3}$, corresponding to concentrations of the order 0.1 at. pct.* Under identical conditions the P and S peaks were generally undetectable on the nonintergranular regions of the fracture surface.

*The high oxygen peak in Figure 9 is related to some surface contamination arising from blisters reaching free surfaces during hydrogen charging.

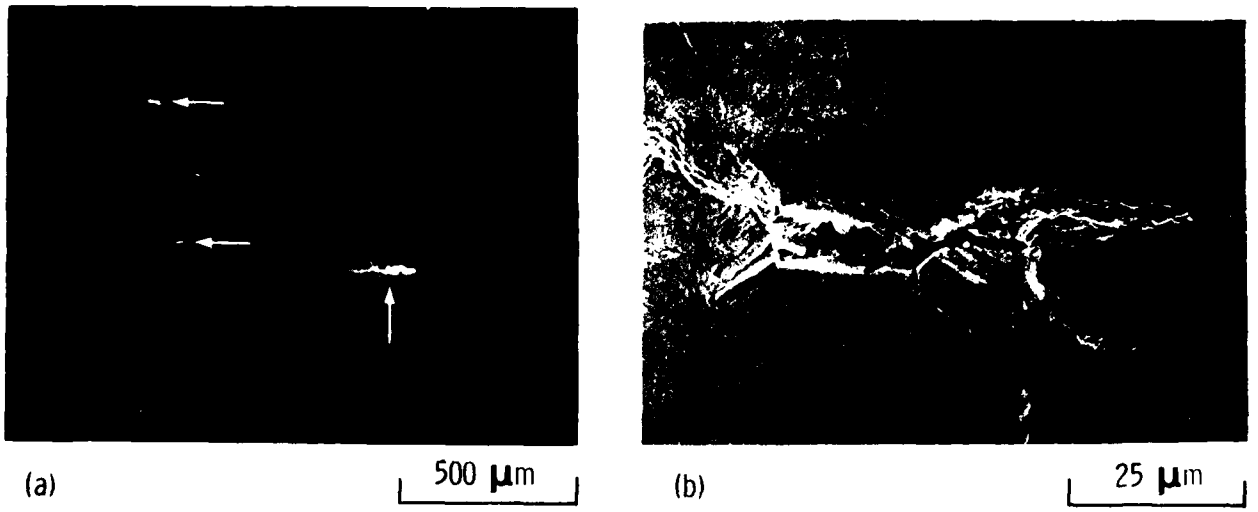

Figure 7. Surface cracks observed in prepolished and etched short-transverse bend specimen of C1-c material. (a) Optical micrograph with arrows indicating cracks in dark bands; oblique illumination, and (b) scanning electron micrograph of surface crack.

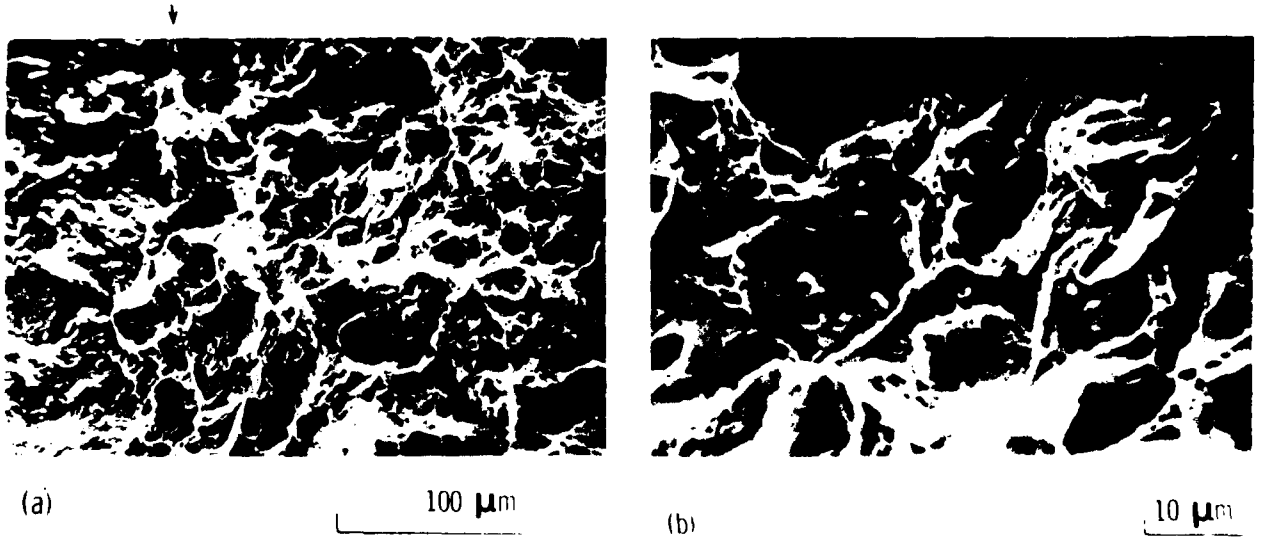

Figure 8. Scanning electron micrographs of fracture surfaces of hydrogen-charged short-transverse notched specimens fractured in vacuum. (a) Fracture surface adjacent to hydrogen blister, showing intergranular facets at center. Flat hydrogen blister is at left of arrows, and (b) intergranular fracture region of (a).

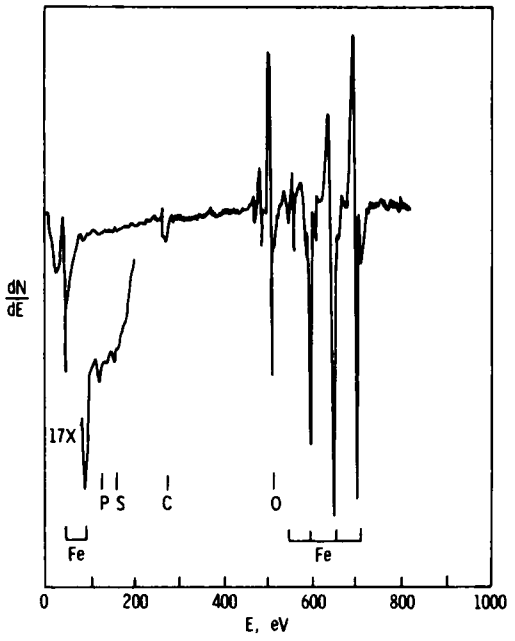

Figure 9. Auger electron spectrum from intergranular fracture region of hydrogen-charged C1-c material fractured in vacuum. 3 kV, 0.9 μA.

EFFECT OF HOMOGENIZATION

Based on the indications that the short transverse embrittlement may be related to impurity segregation in the banded microstructure, the influence of homogenization treatment on the mechanical behavior was investigated. Two 5"x4" sections, 4-1/2 in. in length, were cut from the C1-b material. One piece was given a brief homogenization treatment at 2350°F for 5-1/2 hours in vacuum, and then both were forged at 2050°F to 2-1/8"x4" to simulate the reduction of the C1-c forging. Metallographic examination revealed banding in both pieces, but identical treatment with Stead's reagent, sensitive to phosphorus, indicated a slight reduction in the intensity of the banding in the homogenization-treated material.

Both longitudinal (L) and short transverse (ST) 0.160-in.-dia. tension specimens were machined from the homogenized (H) and nonhomogenized (N) material and given the standard heat treatment. Due to the evidence for a role of environmental interaction in the embrittlement, tension tests were run in a controlled humidity environment at 30% and 85% relative humidity, at a strain rate of 0.002 $min.^{-1}$ Tests were also run in distilled water, and in vacuum after thorough cleaning in alcohol. The results are summarized in Table 5 and the RA is plotted in Figure 10 as a function of humidity. The ST ductility of the nonhomogenized material is strongly influenced by humidity, giving a normal level of ductility when tested in vacuum. The L ductility of both H and N material is relatively insensitive to humidity, while all the material is embrittled in water. The homogenization treatment very nearly restores the ST ductility to that of the longitudinal specimens, thereby eliminating the anisotropic embrittlement.

The influence of homogenization treatment on the sharp crack stress-corrosion behavior was examined in precracked ST specimens under constant load in 3-1/2% NaCl solution, and the results are shown in Figure 11. A K_{ISCC} value of 11 $ksi\sqrt{in.}$ is found for both the H and N material and is identical to that reported for longitudinal specimens

of ESR-processed material of the same hardness level.* Hence the sharp crack stress-corrosion behavior does not appear to reflect the sensitivity to either direction or degree of homogeneity exhibited by the smooth bar tension tests.

Table 5. INFLUENCE OF HOMOGENIZATION ON TENSILE PROPERTIES IN CONTROLLED ENVIRONMENT $\dot{\epsilon}$ = 0.002 min^{-1}

Relative Humidity	Specimen Direction	Condition*	N	UTS, ksi	% RA	Standard Deviation
0% (vacuum).	L	N	3	302	40.8	±2.2
		H	3	301	46.5	±0.6
	ST	N	6	307	36.7	±3.4
		H	4	307	40.6	±1.1
30%	L	N	4	301	40.6	±2.3
		H	4	299	41.3	±3.0
	ST	N	6	303	26.5	±7.3
		H	6	302	40.0	±2.6
85%	L	N	4	298	41.6	±2.1
		H	4	302	43.1	±2.9
	ST	N	5	300	9.4	±5.2
		H	6	303	37.4	±3.0
100% (dist. H_2O)	L	N	4	299	7.5	±4.0
		H	4	292	12.1	±2.8
	ST	N	4	269	5.6	±1.5
		H	2	290	6.5	±2.5

*N = Nonhomogenized
H = Homogenized

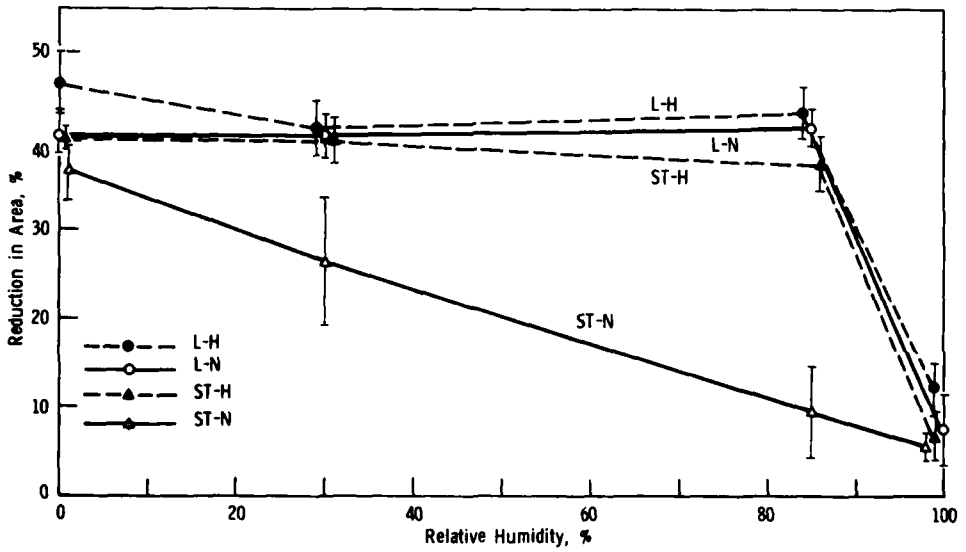

Figure 10. Influence of relative humidity on longitudinal and short-transverse ductility of homogenized (H) and non-homogenized (N) material from heat C1. $\dot{\epsilon}$=0.002 $min.^{-1}$.

*CZYRKLIS, W. F., and LEVY, M. Army Materials and Mechanics Research Center, unpublished research, 1980.

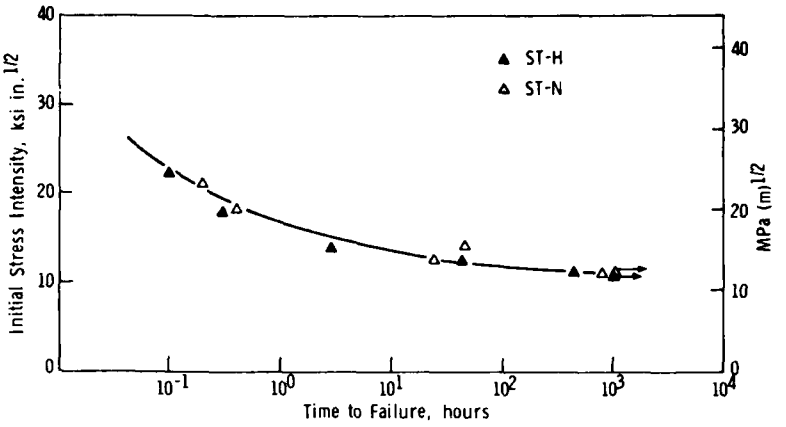

Figure 11. Stress intensity factor K versus time to failure for precracked short-transverse stress corrosion specimens of homogenized (H) and non-homogenized (N) material from heat C1; tested in 3½% NaCl.

DISCUSSION

The anisotropic embrittlement observed here can be understood in terms of the interaction of nonequilibrium segregation inherited from solidification with local equilibrium segregation at grain boundaries during austenitization. Since the extent of grain boundary impurity segregation is strongly dependent on the local composition, the presence of banding can produce local regions with grain boundary segregation characteristic of an alloy of much higher impurity content, as indicated schematically in Figure 12. It is well established that impurities like P, S, and Sn weaken the grain boundaries and increase their sensitivity to environmental interaction,[5] and that relatively small amounts of segregation during austenitizing can cause embrittlement effects

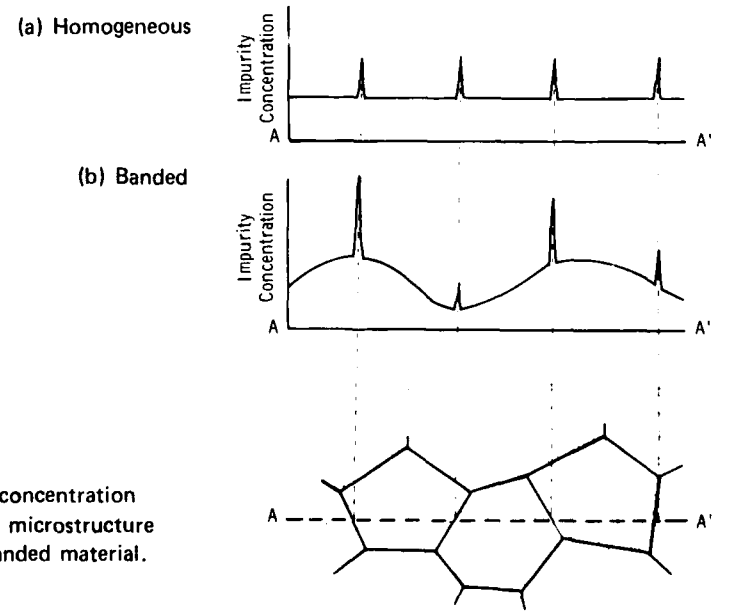

Figure 12. Schematic impurity concentration profiles along line A-A' of lower microstructure for (a) homogeneous, and (b) banded material.

5. BRIANT, C. L., and BANERJI, S. K. *Intergranular Failure in Steel: The Role of Grain Boundary Composition.* Int. Metall. Rev., v. 23, 1978, p. 164-199.

at very high strength levels as observed, for example, in the case of tempered martensite embrittlement.[6] If sufficiently weakened boundaries exist only in the bands, then embrittlement will be most severe when the material is stressed normal to the plane of banding in which aligned arrays of impurity-rich boundaries can act as potent embrittling defects.

Evidence for the interaction of the two types of segregation as depicted in Figure 12 has been obtained recently by Kameda and McMahon[7] in a 0.3C-Ni-Cr steel tempered to hardness of HRC 30. Banded Sb-doped steels showed enhanced intergranular segregation of Sb and associated temper embrittlement relative to homogenized material, although a similar effect could not be detected in their steel when doped with Sn or P.

Anomalous stress-corrosion cracking behavior associated with banding has been observed during tension testing in air in 350-grade maraging steel when aged at low temperatures;[8] premature tensile failures were accounted for via linear-elastic fracture mechanics. In brittle high-strength steels, only a small amount of crack growth during loading is necessary to induce brittle fracture without measurable macroscopic ductility. The critical (surface) flaw size a_c at the yield stress σ_y can be expressed by[9]

$$\frac{a_c}{Q} = \frac{K_{IC}^2}{1.21\pi\ \sigma_y^2} \tag{1}$$

where Q is a shape factor of order unity. Using $K_{IC} \simeq 50$ ksi$\sqrt{\text{in.}}$ and $\sigma_y = 220$ ksi for the ESR 4340 steel gives a critical flaw size of $\sim$0.01 in. in agreement with the extent of intergranular cracking observed in the tension specimens exhibiting completely brittle behavior.

If a number of surface defects, N_A per unit area, is randomly distributed spatially (though nonrandomly oriented), the probability p that the surface of a specimen with gage section surface area A will contain such a defect is expressed by a Poisson function

$$p = 1 - \exp\ (-N_A \cdot A). \tag{2}$$

From the fractions of short transverse 0.252-in. and 0.160-in.-dia. tension specimens of forging C1-c exhibiting significantly premature failure (7/8 and 5/7, respectively), (2) gives $N_A = 2$ in.$^{-2}$ for the controlling defects. These sparsely distributed defects would correspond to impurity-rich regions sufficiently large to allow rapid stress-corrosion cracking over a spatial extent equal to the critical flaw size of $\sim$0.01 in. To act as surface defects in a tension test, such regions must be located within $\delta \simeq 0.01$ in. of the specimen surface. We can then estimate the number of such impurity-rich regions per unit volume as $N_V = N_A/\delta = 2 \times 10^2$ in.$^{-3}$. Estimating plastic zone size R_p from the relation:

$$R_p \simeq \frac{1}{2\pi} \left(\frac{K_I}{\sigma_y}\right)^2 \tag{3}$$

6. BANERJI, S. K., McMAHON, C. J., Jr., and FENG, H. C. *Intergranular Fracture in* 4340-Type *Steels: Effects of Impurities and Hydrogen.* Met. Trans. A, v. 9A, 1978, p. 237-247.
7. KAMEDA, J., and McMAHON, C. J., Jr. *The Effects of Sb, Sn, and P on the Strength of Grain Boundaries in a Ni-Cr Steel.* Met. Trans. A, v. 12A, 1981, p. 31-37.
8. CARTER, C. S. *The Effect of Heat Treatment on the Fracture Toughness and Subcritical Crack Growth Characteristics of a 350-Grade Maraging Steel.* Met. Trans., v. 1, 1970, p. 1551-1559.
9. TIFFANY, C. F., and MASTERS, J. N. *Applied Fracture Mechanics.* ASTM STP 381, 1965, p. 249-278.

gives plastic zone volumes of 1.5×10^{-4} in.^{3} and 8.1×10^{-8} in.^{3} for our K_{IC} and K_{ISCC} specimens. The probability of encountering a defect in the plastic zone of these specimens is then 2.5×10^{-2} and 1.3×10^{-5}, respectively. Hence the lack of abnormal (anisotropic) behavior in the sharp crack tests is consistent with the sparseness of the defects which account for the anomalous behavior of the tension specimens. If the same defects causing stress-corrosion cracking at tension specimen surfaces can cause intergranular fracture under impact conditions, the $\approx 10^{-2}$ in.^{3} plastic zone of a Charpy bar represents sufficient volume to contain such defects accounting for the anisotropy of Charpy impact energies. A similar discrepancy between the behavior of sharp-crack and blunt-notch specimens has been noted in studies of the influence of high austenitizing temperatures on toughness.[10] It is clear from these results that sharp-crack tests cannot be expected to adequately characterize the fracture behavior of inhomogeneous materials; embrittlement phenomena such as that considered here will require tests which sample a sufficient volume of material to incorporate the operative defects.

While the results shown in Figure 1 demonstrate that embrittlement is most severe in heats such as A1 and A2 which have abnormal impurity contents, it is clear that embrittlement is also present (at high hardness levels) in heats like A3 and C1 which show no such compositional abnormalities. Although it is quite improbable that one of the highly potent defects responsible for premature tensile failures could be found in the small specimens on which the Auger analysis was run, one might expect to find less potent examples of the same underlying segregation phenomenon. The Auger results then suggest that the segregation of phosphorus and sulfur is primarily responsible for embrittlement in the heats of "normal" composition.

The sparseness of the potent defects suggests an origin in a solidification segregation phenomenon of coarser size scale than normal microsegregation. A defect density of 10^2 in.$^{-3}$ might be more characteristic of macrosegregation phenomena such as the "channel" defects or "freckles" attributed to gravitationally-induced instabilities in interdendritic fluid flow.[11,12] An issue of concern throughout this investigation has been whether the embrittlement phenomenon is peculiar to, or enhanced by, ESR processing. While it is not at all clear at this time whether ESR promotes channel-type segregates or other such macrosegregation phenomena relative to other ingot processes, the results from heat E (Table 3) indicate that the anisotropic embrittlement can be found in VIM material as well. Similar behavior has also been encountered in conventionally air-melted armor steel (RHA).* There is currently little basis for comparison with other processes such as vacuum arc remelting (VAR) due to the unusually high hardness level of interest here and the general lack of short transverse property data. Further studies are planned involving a split-heat comparison of ESR and VAR materials.

It is well established that the same grain-boundary impurity segregants responsible for brittle intergranular fracture under impact conditions promote intergranular stress-corrosion cracking.[5] There is also mounting evidence that the underlying mechanism of stress-corrosion cracking in high-strength martensitic steels is hydrogen embrittlement through cathodic charging at the crack tip.[13] Failures related to internal hydrogen in

*DeSISTO, T. S., ANCTIL, A. A., and KULA, E. B. Army Materials and Mechanics Research Center, unpublished research, 1977.

10. RITCHIE, R. O., FRANCIS, B., and SERVER, W. L. *Evaluation of Toughness in AISI 4340 Alloy Steel Austenitized at Low and High Temperatures.* Met. Trans. A, v. 7A, 1976, p. 831-838.
11. FLEMINGS, M. C. *Principles of Control of Soundness and Homogeneity of Large Ingots.* Scandinavian Journal of Metallurgy, v. 5, 1976, p. 1-15.
12. MEHRABIAN, R., KEANE, M. A., and FLEMINGS, M. C. *Experiments on Macrosegregation and Freckle Formation.* Met. Trans. , v. 1, 1970, p. 3238-3241.
13. SANDOZ, G. *A Unified Theory for Some Effects of Hydrogen Source, Alloying Elements, and Potential on Crack Growth in Martensitic AISI 4340 Steel.* Met. Trans., v. 3, 1972, p. 1169-1176.

plated helicopter components may thus reflect the same basic embrittlement mechanism, consistent with the intergranular fracture of the hydrogen-charged specimens on which the Auger analysis was performed. Regardless of the source of hydrogen, internal or external, the same microstructural defects can be expected to control failure. Anisotropy of internal hydrogen embrittlement behavior will be investigated in the planned ESR-VAR comparative study.

Whatever the exact origin of the impurity-rich defects encountered in this study, it is clear the homogenization treatment is a viable approach to their mitigation. Based on the measured diffusivity of phosphorus in austenite[14] and the interband distance in the forgings, the brief homogenization treatment applied to the C1 material (Figure 10) would be more than sufficient to homogenize phosphorus if it were the only diffusing species. The treatment would not be sufficient to homogenize the slower-diffusing alloy elements like Ni and Mn, which can promote cosegregation of boundary impurities.[15] The results of Figure 10 indicate, however, that the degree of homogenization obtained is sufficient to restore very nearly isotropic properties.

The improvement of properties in the C1-d material forged at 2300°F is likely also due to some homogenization. An investigation of "overheating" effects related to dissolution of sulfides and reprecipitation on grain boundaries revealed that this form of embrittlement is encountered over a very limited range of cooling rates in this steel,[16] and the associated dimpled intergranular fracture is quite distinct from the smooth intergranular fracture observed here. In addition, anisotropy of overheating embrittlement has been found to be the opposite of that encountered here.[3]

A study by Rao[4] of the influence of homogenization treatment on the transverse mechanical properties of 4340 bar material tempered at 1050°F (∿HRC 37 hardness) showed a 10% to 20% improvement in Charpy impact energy, and a 5% to 7% increase in reverse bending (R=-1) fatigue strength. These are rather modest improvements relative to the cost of homogenization, and homogenization treatment is generally viewed as unnecessary for applications of 4340 at conventional hardness levels. In contrast, the lack of a homogenization treatment at the HRC 55 hardness level of interest here is catastrophic, due to the greatly enhanced sensitivity to impurities in martensitic steels at high-strength levels. If other desirable properties such as ballistic tolerance require the use of these steels at extreme hardness levels, then homogenization, either by suppression of initial segregation or by subsequent heat treatment, is absolutely essential.

CONCLUSIONS

The anisotropic embrittlement of high hardness ESR 4340 steel forgings is attributed to an interaction of nonequilibrium segregation on solidification with local equilibrium grain boundary segregation during austenitizing to produce defective regions of enhanced grain-boundary impurity segregation which are oriented during forging. The segregated impurities, primarily phosphorus and sulfur, cause intergranular fracture under impact conditions and abnormal sensitivity to environmental attack during low strain rate deformation. The defective regions are sparsely distributed such that the anisotropic embrittlement is encountered only in tests which sample a sufficient volume of material, i.e., smooth-bar tension and blunt-notched toughness tests; the anisotropy is absent in sharp-crack tests. Isotropic properties are restored by a homogenization treatment. For application of such steels at extreme hardness levels, homogenization is essential.

14. SEIBEL, G. *Diffusion du phosphore dans le fer.* Academie des Sciences Comptes Rendus, 256, 1963, p. 4661.
15. GUTTMAN, M. *Equilibrium Segregation in a Ternary Solution: A Model for Temper Embrittlement.* Surf. Sci., v. 53, 1975, p. 213-227.
16. BOLDY, M. D., FUJII, T., POURIER, D. R., and FLEMINGS, M. C. *Sulfide Inclusions in Electroslag Remelted Steels.* Massachusetts Institute of Technology, Final Report, Contract DAAG46-78-C-0032, AMMRC TR 81-4, January 1981.

DISTRIBUTION LIST

No. of Copies	To
1	Office of the Under Secretary of Defense for Research and Engineering, The Pentagon, Washington, DC 20301
12	Commander, Defense Technical Information Center, Cameron Station, Building 5, 5010 Duke Street, Alexandria, VA 22314
	Metals and Ceramics Information Center, Battelle Columbus Laboratories, 505 King Avenue, Columbus, OH 43201
1	ATTN: J. H. Brown, Jr.
	Deputy Chief of Staff, Research, Development, and Acquisition, Headquarters, Department of the Army, Washington, DC 20310
1	ATTN: DAMA-ARZ
	Commander, Army Research Office, P.O. Box 12211, Research Triangle Park, NC 27709
1	ATTN: Information Processing Office
	Commander, U.S. Army Materiel Development and Readiness Command, 5001 Eisenhower Avenue, Alexandria, VA 22333
1	ATTN: DRCLDC
	Commander, U.S. Army Materiel Systems Analysis Activity, Aberdeen Proving Ground, MD 21005
1	ATTN: DRXSY-MP, Director
	Commander, U.S. Army Missile Command, Redstone Arsenal, AL 35809
1	ATTN: Technical Library
1	DRSMI-CS, R. B. Clem
	Commander, U.S. Army Armament Research and Development Command, Dover, NJ 07801
2	ATTN: Technical Library
1	DRDAR-SCM, J. D. Corrie
1	Dr. J. Frasier
	Commander, U.S. Army Tank-Automotive Research and Development Command, Warren, MI 48090
1	ATTN: DRDTA-RKA
2	DRDTA-UL, Technical Library
1	DRDTA-RCK, Dr. J. Chevalier
	Commander, U.S. Army Foreign Science and Technology Center, 220 7th Street, N.E., Charlottesville, VA 22901
1	ATTN: Military Tech, Mr. Marley
	Director, Eustis Directorate, U.S. Army Air Mobility Research and Development Laboratory, Fort Eustis, VA 23604
1	ATTN: DAVDL-E-MOS
1	DAVDL-EU-TAP
	U.S. Army Aviation Training Library, Fort Rucker, AL 36360
1	ATTN: Building 5906--5907
	Commander, U.S. Army Aviation Research and Development Command, 4300 Goodfellow Boulevard, St. Louis, MO 63120
1	ATTN: DRDAV-EGX
1	DRDAV-EX, Mr. R. Lewis
1	DRDAV-EQ, Mr. Crawford
1	DRCPM-AAH-TM, Mr. R. Hubbard
1	DRDAV-DS, Mr. W. McClane
	Naval Research Laboratory, Washington, DC 20375
1	ATTN: Dr. J. M. Krafft - Code 5830
1	Code 2627
	Chief of Naval Research, Arlington, VA 22217
1	ATTN: Code 471

No. of Copies	To
	Director, Structural Mechanics Research, Office of Naval Research, 800 North Quincy Street, Arlington, VA 22203
1	ATTN: Dr. N. Perrone
	Commander, U.S. Air Force Wright Aeronautical Laboratories, Wright-Patterson Air Force Base, OH 45433
2	ATTN: AFWAL/MLSE, E. Morrissey
1	AFWAL/MLC
1	AFWAL/MLLP, D. M. Forney, Jr.
1	AFWAL/MLBC, Mr. Stanley Schulman
1	AFWAL/MLXE, A. Olevitch
	National Aeronautics and Space Administration, Washington, DC 20546
1	ATTN: Mr. B. G. Achhammer
1	Mr. G. C. Deutsch - Code RW
	National Aeronautics and Space Administration, Marshall Space Flight Center, Huntsville, AL 35812
1	ATTN: R. J. Schwinghammer, EH01, Dir, M&P Lab
1	Mr. W. A. Wilson, EH41, Bldg. 4612
	Chief of Naval Operations, Washington, DC 20350
1	ATTN: OP-987, Director
	Aeronautical Systems Division (AFSC), Wright-Patterson Air Force Base, OH 45433
1	ATTN: ASD/ENFEF, D. C. Wight
1	ASD/ENFTV, D. J. Wallick
1	ASD/XRHD, G. B. Bennett
	Air Force Armament Laboratory, Eglin Air Force Base, FL 32542
1	ATTN: AFATL/DLYA, V. D. Thornton
	Air Force Flight Dynamics Laboratory, Wright-Patterson Air Force Base, OH 45433
1	ATTN: AFFDL/FES, G. W. Ducker
1	AFFDL/FES, J. Hodges
1	AFFDL/TST, Library
	Air Force Test and Evaluation Center, Kirtland Air Force Base, NM 87115
1	ATTN: AFTEC-JT
	Armament Development and Test Center, Eglin Air Force Base, FL 32542
1	ATTN: ADTC/TS
	NASA - Ames Research Center, Mail Stop 223-6, Moffett Field, CA 94035
1	ATTN: SC, J. Parker
	NASA - Ames Research Center, Army Air Mobility Research and Development Laboratory, Mail Stop 207-5, Moffett Field, CA 94035
1	ATTN: SAVDL-AS-X, F. H. Immen
	NASA - Johnson Spacecraft Center, Houston, TX 77058
1	ATTN: JM6
1	ES-5
	Naval Air Development Center, Warminster, PA 18974
1	ATTN: Code 063
	Naval Air System Command, Department of the Navy, Washington, DC 20360
1	ATTN: AIR-03PAF
1	AIR-5203
1	AIR-5204J
1	AIR-530313
	Naval Material Command, Washington, DC 20360
1	ATTN: MAT-0331
	Naval Post Graduate School, Monterey, CA 93948
1	ATTN: Code 57BP, R. E. Ball

No. of Copies	To
	Naval Surface Weapons Center, Dahlgren Laboratory, Dahlgren, VA 22448
1	ATTN: Code G-54, Mr. J. Hall
1	Code G-54, Mr. E. Rowe
	Naval Weapons Center, China Lake, CA 93555
1	ATTN: Code 40701
1	Code 3624, Mr. C. A. Johnson
	Commander, Rock Island Arsenal, Rock Island, IL 61299
1	ATTN: DRSAR-PPV
	Armament Systems, Inc., 712-F North Valley, Anaheim, CA 92801
1	ATTN: J. Musch
	Beech Aircraft Corporation, 9709 E. Central Avenue, Wichita, KS 67206
1	ATTN: Engineering Library
	Bell Helicopter Company, A Textron Company, P.O. Box 482, Fort Worth, TX 76101
1	ATTN: J. R. Johnson
	Boeing Vertol Company, A Division of the Boeing Company, P.O. Box 16858, Philadelphia, PA 19 19142
1	ATTN: J. E. Gonsalves, M/S P32-19
	Calspan Corporation, P.O. Box 235, Buffalo, NY 14221
1	ATTN: Library
	Cessna Aircraft Company, Wallace Division, P.O. Box 1977, Wichita, KS 67201
1	ATTN: B. B. Overfield
	Fairchild Industries, Inc., Fairchild Republic Company, Conklin Street, Farmingdale, Long Island, NY 11735
1	ATTN: Engineering Library, G. A. Mauter
	Falcon Research and Development Company, 601 San Pedro, N.E., Suite 205, Albuquerque, NM 87108
1	ATTN: W. L. Baker
	General Dynamics Corporation, Convair Division, P.O. Box 80877, San Diego, CA 92138
1	ATTN: Research Library, U. J. Sweeney
	General Research Corporation, Science and Technology Division, 5383 Hollister Avenue, P.O. Box 3587, Santa Barbara, CA 93105
1	ATTN: R. Rodman
	Gruman Aerospace Corporation, South Oyster Bay Road, Bethpage, NY 11714
1	ATTN: Technical Information Center, J. Davis
	Hughes Helicopters, A Division of Summa Corporation, Centinela & Teale Street, Culver City, CA 90230
1	ATTN: Library, 2/T2124, D. K. Goss
1	Mr. A. Hirko
1	Mr. L. Soffa
1	Mr. A. Edwards
	IIT Research Institute, 10 West 35th Street, Chicago, IL 60616
1	ATTN: K. McKee
	Kaman Aerospace Corporation, Old Winsor Road, Bloomfield, CT 06002
1	ATTN: H. E. Showalter
	Lockheed-California Company, A Division of Lockheed Aircraft Corporation, Burbank, CA 91503
1	ATTN: Technological Information Center, 84-40, U-35, A-1
	Vought Corporation, P.O. Box 5907, Dallas, TX 75232
1	ATTN: D. M. Reedy, 2-30110
1	M. P. Poullos, Jr.
	Martin Marietta Corporation, Orlando Division, P.O. Box 5837, Orlando, FL 32805
1	ATTN: Library, M. C. Griffith

No. of Copies	To
	McDonnell Douglas Corporation, 3855 Lakewood Boulevard, Long Beach, CA 90846
1	ATTN: Technical Library, C1 290/36-84
	Northrop Corporation, Aircraft Division, 3901 W. Broadway, Hawthorne, CA 90250
1	ATTN: Mgr. Library Services, H. W. Jones
	Parker Hannifin Corporation, Bertea Control Systems Division, 18001 Von Karman Avenue, Irvine, CA 92715
1	ATTN: C. Beneker
	Rockwell International Corporation, Los Angeles Aircraft Division, B-1 Division, International Airport, Los Angeles, CA 90009
1	ATTN: W. L. Jackson
	Sikorsky Aircraft, A Division of United Aircraft Corporation, Main Street, Stratford, CT 06602
1	ATTN: J. B. Faulk
1	W. G. Dignam
	Teledyne CAE, 1330 Laskey Road, Toledo, OH 43697
1	ATTN: Librarian, M. Dowdell
	Simonds Steel Division, Guterl Special Steel Corporation, Lockport, NY 14094
1	ATTN: Mr. R. Farrington
	Atlas Testing Laboratories, Inc., 6929 E. Slauson Avenue, Los Angeles, CA 90040
1	ATTN: Mr. P. S. Horvath
	Georgia Institute of Technology, School of Mechanical Engineering, Atlanta, GA 30332
1	ATTN: Dr. J. T. Berry
	Lukens Steel Company, Coatesville, PA 19320
1	ATTN: Dr. R. S. Swift
	Republic Steel Corporation, 410 Oberlin Avenue SW, Massillon, OH 44646
1	ATTN: Mr. R. Sweeney
1	Mr. W. H. Brechtel
1	Mr. B. G. Hughes
	Boeing Commercial Airplane Company, P.O. Box 3707, MS73-43, Seattle, WA 98124
1	ATTN: Dr. K. White
	United States Steel Corporation, Research Laboratory, Monroeville, PA 15146
1	ATTN: Dr. Hsun Hu
	METTEC, 1805 E. Carnegie Avenue, Santa Ana, CA 92705
1	ATTN: Dr. L. Raymond
	Ingersoll Rand Oilfield Products Division, P.O. Box 1101, Pampa, TX 79065
1	ATTN: Mr. W. L. Hallerberg
	Brown University, Division of Engineering, Providence, RI 02912
1	ATTN: Prof. J. Duffy
	SRI International, 333 Ravenswood Avenue, Menlo Park, CA 94025
1	ATTN: Dr. D. Shockey
	Director, Army Materials and Mechanics Research Center, Watertown, MA 02172
2	ATTN: DRXMR-PL
4	Authors


DATE
ILME